Tutorial: high-flux electron gun reference design
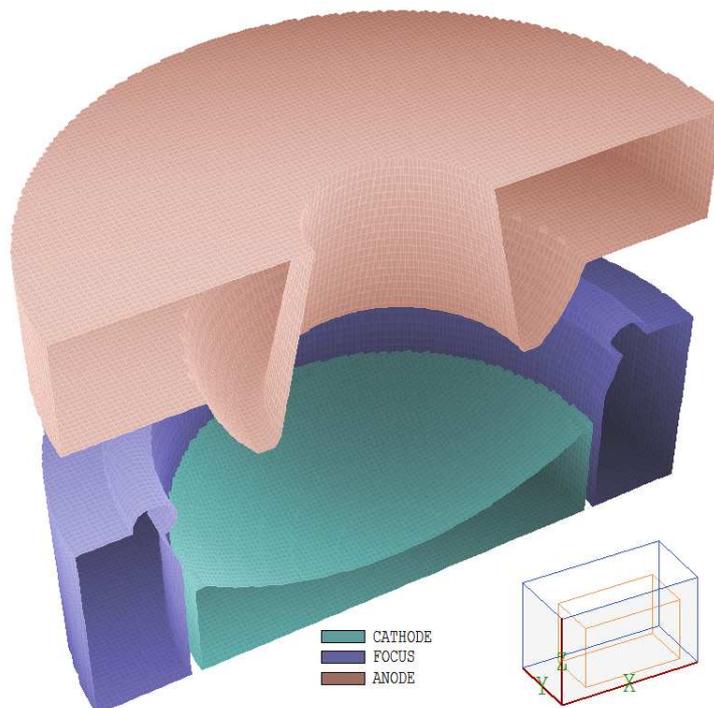
Stanley Humphries, Copyright 2010

Figure 1: Three-dimensional cutaway view of the 3.2 μperv electron gun.

This tutorial addresses a common issue in electron gun design: for a given voltage, what is the highest possible beam current? By electron gun, I mean a conventional circular device. A sheet beam injector could extend without limit in the long direction and generate infinite current. Furthermore, I limit consideration to guns with an anode aperture rather than a grid. Gridded guns could achieve extremely high current, but the resulting beam cannot propagate because of longitudinal space-charge effects. Also, gridded guns are limited to low duty cycle. Finally, the results presented apply to non-relativistic injectors in the energy range ≤ 50 keV. Such a gun could be used as the initial stage of a high-voltage accelerator.

Sections 7.1 through 7.4 of my book **Charged Particle Beams** (available for download at `http://www.fieldp.com/cpb.html`) give a detailed discussion of the principles underlying high-current electron gun design. Here, I will summarize some of the main points. The maximum electron current density that can be accelerated across a planar gap of infinite transverse dimension is given by the Child law:

$$j_e = \left[\frac{4\epsilon_0}{9}\right] \sqrt{\frac{2e}{m_e}} \, \frac{V_0^{3/2}}{d^2}. \tag{1}$$

The expression is in SI units, with d the gap width in meters and V_0 the

applied voltage in volts. Substituting values for physical constants gives the practical expression:

$$j_e = 2.33 \times 10^{-6} \ \frac{V_0^{3/2}}{d^2}. \tag{2}$$

The units are A/m^2 for d in m and A/cm^2 for d in cm.

An anode grid would be necessary to extract a beam from a uniform planar gap. Introducing an aperture of radius R_a eliminates a portion of the anode plane. There are two consequences if R_a is comparable to or larger than d:

- The reduced electric field near the cathode center lowers local current density and net current. Because the cathode temperature must be sufficient to supply the space-charge-limited current density at the edge, the source is used inefficiently.

- Nonlinear electrostatic focusing forces near the aperture edge lead to non-laminar orbits in the extracted beam.

If we impose the limit $R_a \leq d/2$, then the extraction area is about $A = \pi d^2/4$. Using Eq. 2, the maximum total current from an electron gun with an aperture is about

$$I \sim 2.33 \times 10^{-6} \ \frac{\pi}{4} \ V_0^{3/2}. \tag{3}$$

The *perveance* of an electron gun is defined as

$$P = \frac{I}{V_0^{3/2}}. \tag{4}$$

Equation 3 implies that the upper limit on perveance for a circular-beam gun is approximately $P \leq 1.9 \times 10^{-6}$ perv or 1.9 μperv. Higher perveance values may can be achieved with a converging-beam gun. Here, a cathode surface with the shape of a spherical section produces a beam with reduced size at the anode, allowing a smaller aperture. The upper limit on perveance for a converging-beam gun depends on the tolerance to beam imperfections. The value is roughly 3 μperv.

This report addresses a reference design for a 3.2 μperv electron gun. It is important to note the universality of the design. The scaling laws inherent in the electrostatic equations and the Child law mean that a single reference design can be applied to all possible non-relativistic electron guns. For example:
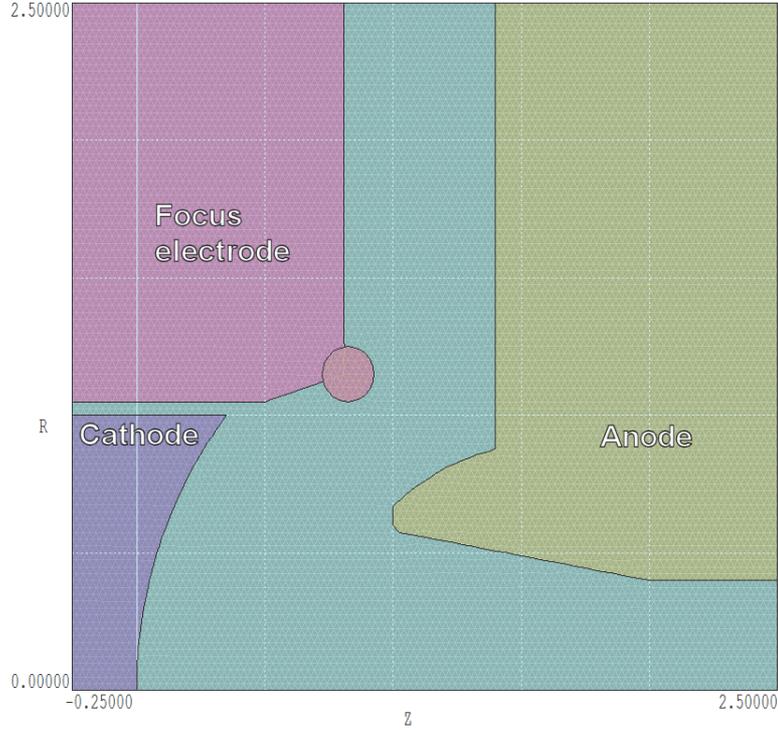
Figure 2: Simulation geometry of the electron gun, r-z projection. Nominal units are cm.

- To change the cathode diameter from R_c to R'_c, multiply all dimensions by (R'_c/R_c).

- To change the current from I_e to I'_e, adjust the voltage by $(I'_e/I_e)^{2/3}$.

- To lower the peak electric field by a factor $(1/\alpha)$, scale all dimensions by α.

The design has good (but not perfect) emitted current-density uniformity and an approximately laminar output beam. The peak electric field magnitude is low, the parts are easy to fabricate, the open structure allows good vacuum pumping and there is a relatively large gap between the cathode and focusing electrode.

The input files (3UPERV) are available to users of the **Trak** code. The geometry defined in 3UPERV.MIN is shown in Figs. 1 and 2. The specific instance has a cathode of radius $R_c = 1.0$ cm. The emission surface at $r = 0.0$ is located at axial position $z = 0.0$ cm. The applied voltage is 20 kV and the target current is 9.0 A. The cathode surface is a spherical section with center at position $z = 1.6R_c$. The section encloses an angle of 38.7º.

4

The focusing electrode (at the same potential as the cathode) serves two purposes:

- Reduction of field enhancement at the cathode edge to prevent a spike in current density.

- Shaping of global electric fields so that all electrons pass through the aperture.

The surface of the focusing electrode in a low-perveance gun is simply a conical section inclined at the Pierce angle (22.5°) with respect to the outer edge of the cathode. There is no set prescription for the electrode shape in a high-perveance gun. The focusing electrode in Fig. 2 was determined by informed trial-and-error. My goals were to maximize clearance between the beam envelope and the aperture edge, to achieve acceptable current-density uniformity and to generate an approximately laminar beam with a waist at the gun exit ($z = 2.5$ cm). Several iterations were necessary because an improvement of one characteristic tended to degrade the others. For example, increasing the aperture radius for more clearance reduced the emitted current density at the cathode center. A larger extension of the focusing electrode to reduce current density on the cathode edge resulted in over-focusing of peripheral electrons. In the end, the design is a compromise, but a useful starting point. Note that the focusing electrode and anode form a simple planar gap at large radius. Modifications can be made to match to different mountings with a relatively small affect on fields in the gun region.

Figure 3 shows model electron orbits in the self-consistent electric field. The emitted current is 9.0 A. There is about 0.7 mm clearance between the beam envelope and the anode extension. The beam reaches a waist of radius 3.5 mm at z = 2.4 cm. As a check, I confirmed that there was little difference in a **Trak** solution with full relativistic effects. Figure 4 shows the phase space distribution at the beam waist. There is some over-focusing of peripheral electrons, giving an RMS angular divergence of 1.31°. The cathode current density as a function of r is plotted in Fig. 5. The quantity varies from 2.0 A/cm² at the center to 3.4 A/cm² at the edge.

The magnitude of the self-consistent electric field is plotted in Fig. 6. Field stress is concentrated at the extensions of the focusing electrode and anode. The peak value is relatively low, ~ 83 kV/cm. The peak space-charge potential in the extracted beam is -860 V, leading to an RMS energy spread of ± 141 keV.Finally, Fig. 7 shows the approximate radial variation of current density in the exit beam. The over-focusing of peripheral electrons gives crossing orbits and an inevitable divergence of current density at the beam envelope. This singular effect would drop off as the beam moves downstream.
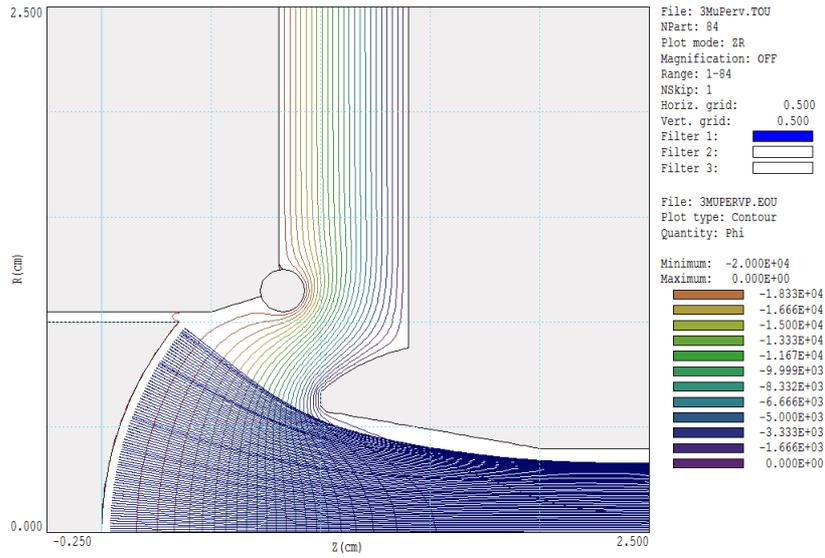
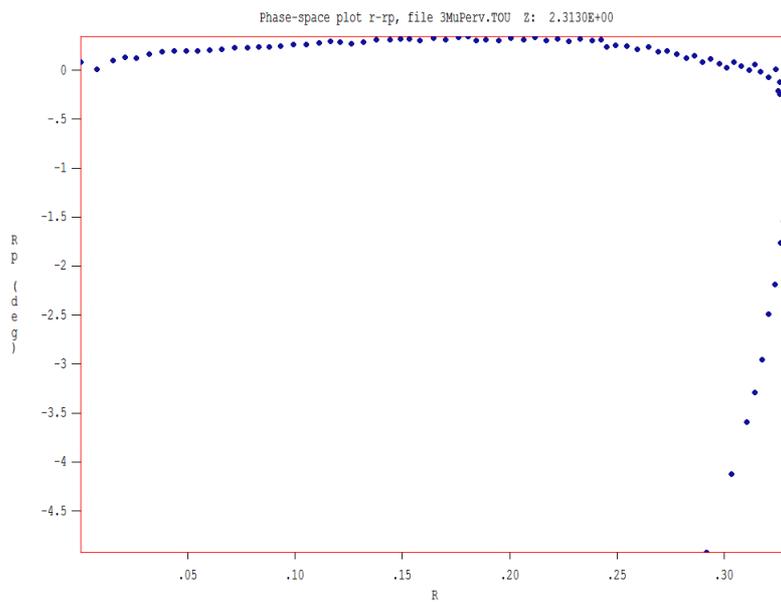Figure 3: Self-consistent model electron trajectories and equipotential lines.

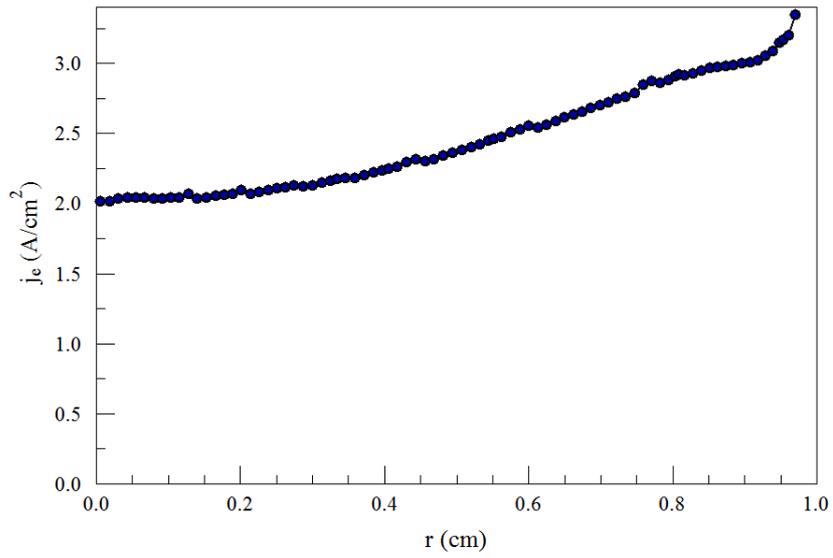Figure 4: Radial phase-space distribution at the beam waist ($z = 2.4$ cm).
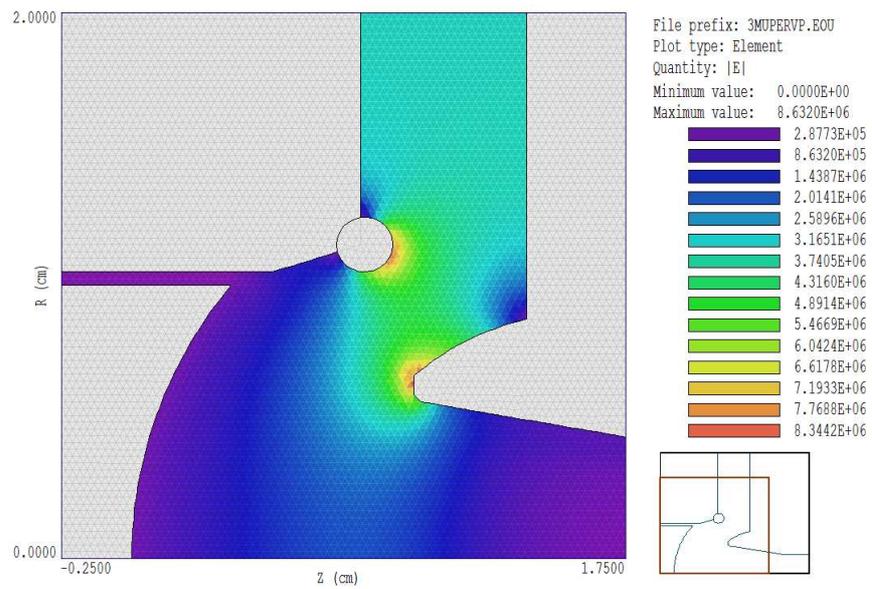
Figure 5: Cathode current density as a function of r.

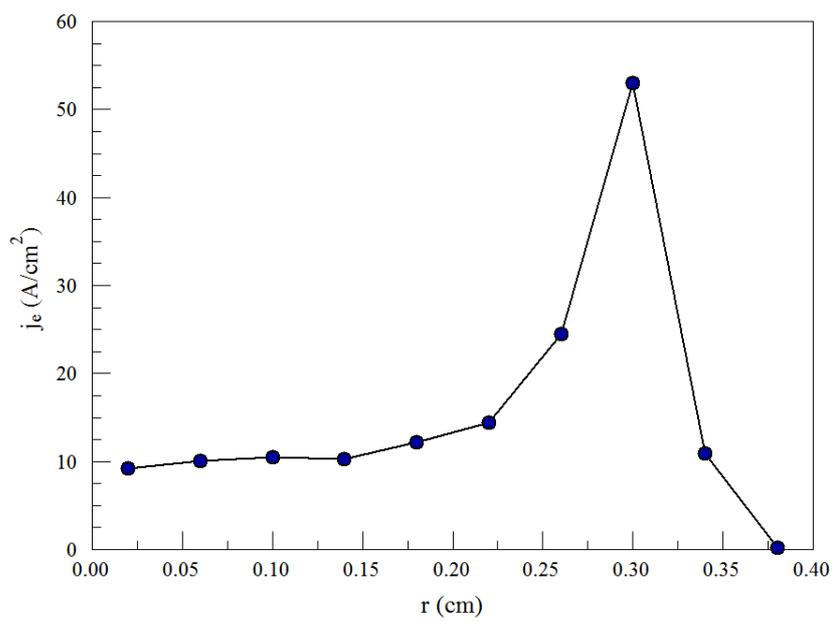Figure 6: Plot of the self-consistent electric field magnitude $|\mathbf{E}|$.

7

Figure 7: Exit beam current density at $z = 2.4$ cm.